JOURNAL OF MATERIALS SCIENCE **38** (2003) 4557–4565

Elimination of Fe in Al-Si cast alloy scrap by electromagnetic filtration

XU ZHENMING*, LI TIANXIAO, ZHOU YAOHE
School of Materials Science and Engineering, and State Key Lab. of MMCs, Shanghai Jiao Tong University, Shanghai 200030, People's Republic of China
E-mail: zmxu@sjtu.edu.cn

Fe in Al-Si cast alloy scrap melt was eliminated by electromagnetic filtration of primary iron-rich phases, which were formed by adding Mn in the melt. The principle of electromagnetic filtration is that the electromagnetic force scarcely acts on the primary iron-rich phases due to its low electric conductivity as compared to the melt. As a result, a repulsive force exerts on the primary iron-rich phases to move them in the direction opposite to that of the electromagnetic force. It has been found that the forming temperature of primary iron-rich phase increases gradually with the increment of ratio of Mn to Fe (Mn/Fe), and that the iron-rich phases are formed as primary phases, they appear as massive particles with size of 30–80 μm. Experimental results show that the primary iron-rich phases are separated from Al-Si alloy scrap melt and are collected in the electromagnetic separation chamber. Fe content in the cast ingot decreases from 1.20% to 0.41% by electromagnetic filtration, which can meet the demand for casting. This new technique is highly efficient and available for continuous processing compared with natural settling and filtration methods. It offers a possibility for recycling high quality aluminum alloys.

Nomenclature

B	magnetic flux density vector, T
J	electric current density, A/m^2
f_p	electromagnetic force acting on the primary iron-rich phase, N/m^3
σ_f	electrical conductivity of the Al-Si alloy melt, Ω^{-1}.m^{-1}
σ_p	electrical conductivity of the primary iron-rich phase, Ω^{-1}.m^{-1}
$2h$	height of the single filtration passage of the separation chamber, m
b	width of the single filtration passage of the separation chamber, m
u	horizontal velocity of Al-Si alloy melt, m/s
u_M	the largest horizontal velocity of the Al-Si alloy melt, m/s
v_t	perpendicular terminal migration velocity of the primary iron-rich phase, m/s
d_p	diameter of the primary iron-rich phase, m
μ	viscosity of the Al-Si alloy melt, Pa.s
η	removal efficiency of primary iron-rich phase, %
P^o	pressure loss of unit Al-Si alloy melt, Pa
ρ	density of Al-Si alloy melt, kg/m^3
ρ_p	density of primary iron-rich phase, kg/m^3
g	gravity acceleration, m/s^2
R_e	Reynolds number of primary iron-rich phase on perpendicular direction
φ	coefficient of resistance
R	resistance acting on the primary iron-rich phase, N/m^3
m	mass of the primary iron-rich phase, kg
$\frac{dv}{dt}$	acceleration of the primary iron-rich phase
W_o	factual gravity of the primary iron-rich phase in the Al-Si alloy melt, N/m^3
x	acting length of electromagnetic force, m

1. Introduction

A crucial technical subject in recycling scraps is how to remove the detrimental elements, which are harmful to the mechanical properties of end products and difficult to be eliminated, e.g., iron in aluminum [1–3]. Usually, it can be eliminated by natural settling [1] and centrifugal methods [3] based on density difference between the melt and the iron-rich phases and by filtration method [2]. However, these methods have significant disadvantages of long treatment time, low efficiency, and most of all, settling and centrifugal methods can not work continuously. Therefore, they are very limited in applications. In electromagnetic filtration the electromagnetic force is exerted on the melt in the separation chamber. Thus, The electromagnetic force scarcely acts on the primary iron-rich phases due to its low electric conductivity, which then moves in the direction opposite to that of the electromagnetic force. As a result, the primary

*Author to whom all correspondence should be addressed.

iron-rich phases are separated from Al-Si alloy scrap melt and are collected in the separation chamber while the melt is in continuous flow. Therefore, the electromagnetic filtration can improve filtrating efficiency as compared with natural filtration method. This method has significant potential advantages of high efficiency, continuous work, and increased cleanliness of the melt. Although the method of electromagnetic separation of iron in static molten Al-Si alloy has been preliminarily studied [4, 5], it can not work continuously. Nagy EI-Kaddah *et al*. [6] have simply studied the removal of (Fe,Mn)-Al intermetallic phase from Al-1Fe-6Mn alloy by an induced-current separator. In this research, the formation of primary iron-rich phases in the Al-Si alloy melt has been studied by settling method and thermal analysis. Furthermore, electromagnetic filtration of primary iron-rich phases has been investigated by theoretical analysis and on a self-designed electromagnetic filtration equipment.

2. Experimental procedure

The chemical compositions of test materials are listed in Table I. Fifty grams of alloy was heated to 800°C within a crucible in a resistance furnace, then the melt was cooled for settling. Settling experiments were carried out every 10°C from 760°C to 600°C. The melt was kept 40 minutes at every settling temperature, then the solidified samples were prepared for observing their metallographic structures. Thermal analysis was also used to determine the forming temperature of the iron-rich phases. Fig. 1 shows a schematic illustration of the electromagnetic filtration system, which consists of an electromagnet, casting mould, an electromagnetic separation chamber and a DC power supply. The size of the electromagnet poles was 130 mm × 130 mm. Structure of the electromagnetic separation chamber is shown in Fig. 2. The various processing parameters for the electromagnetic filtration were as follows:

(1) The temperature of the alloy melt was 720°C;
(2) The space distance between two magnetic poles was 40–120 mm, and the magnetic flux density was 0–1 T;
(3) The direct electric current intensity in the melt was 0–2.0 × 10^5 A/m^2;
(4) The weight of the melt was 5 kg.

TABLE I Chemical compositions of test materials (wt%)

Mark	Fe	Mn	Si	Al	Mn/Fe
A-0.0	1.2	0.0	11.7	Bal.	0.0
A-0.5	1.2	0.6	11.7	Bal.	0.5
A-1.0	1.2	1.2	11.7	Bal.	1.0
A-1.5	1.2	1.8	11.7	Bal.	1.5
A-2.0	1.2	2.4	11.7	Bal.	2.0

3. Results and discussion

3.1. Formation of primary iron-rich phases in Al-Si alloy melt

Fig. 3 shows the effect of Mn on the microstructures of Al-Si-1.2 wt%Fe alloys. It is seen that the morphology of the iron-rich phases (compounds) changes from long needle-like (Fig. 3a) into long needle-like particles and massive particles (Fig. 3b) with increasing of Mn/Fe ratio. When Mn/Fe is equal to 1.5, the needle-like iron compounds become completely massive (Fig. 3c). The change in the morphology of iron phases is due to the transformation of needle-like β iron compounds ($Al_9Fe_2Si_2$) into massive α iron compounds (AlSiFeMn). The chemical compositions of massive α iron compound are (wt%): Al-54.26, Si-10.72, Mn-22.97, Fe-17.04 as determined by electroprobe analysis.

Fig. 4 shows the cooling curves of Al-Si-1.2 wt%Fe and Al-Si-1.2 wt%Fe-1.8 wt%Mn. From Fig. 4, it can be seen that the primary crystallization temperature of primary iron-rich phases (iron compounds) is 735°C. Fig. 5 shows the settling results at each marked point on the cooling curve. It can be seen that the amount of the primary massive iron-rich phase increases gradually with decreasing settling temperature. When the settling temperature is 680°C, large particles of iron-rich phases are present owing to conglomeration during settling, as shown in Fig. 5c. Some times the size of the primary iron-rich phase is 30–80 μm after adding Mn. The relationship between primary crystallizing temperature and Mn/Fe is obtained by thermal analysis and settling tests, as shown in Fig. 6. The forming temperature of the iron compound increases gradually with the increment of Mn/Fe because the forming temperature of α iron compounds (AlSiFeMn) is higher than that of needle-like β iron compounds ($Al_9Fe_2Si_2$) [1]. The

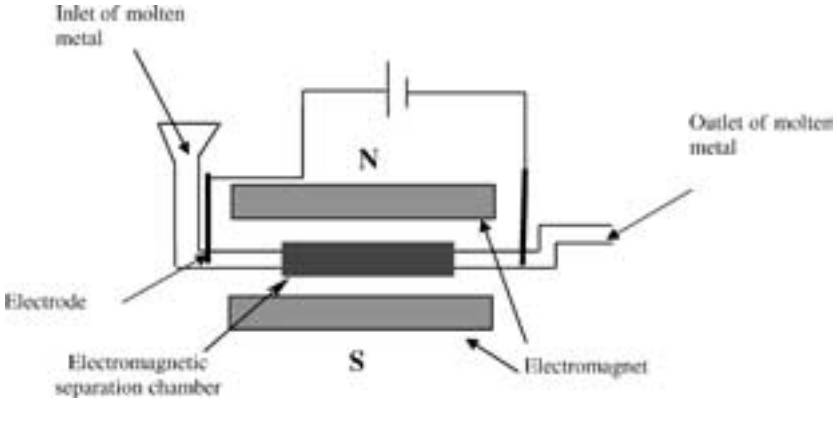

Figure 1 Sketch of experimental apparatus.

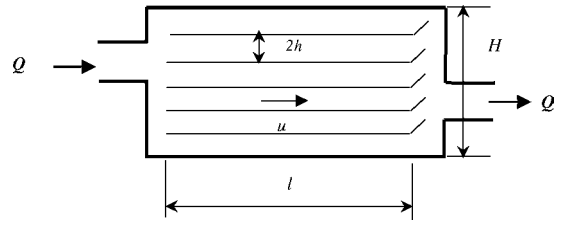

Figure 2 Structure of the electromagnetic separation chamber.

region of the forming temperature of iron-rich phase is 680–735°C, and is above the eutectic temperature (570°C) of the alloy when Mn/Fe is over 1.0. Since the iron compounds are formed primarily after adding Mn, it is possible to separate iron-rich phases from the melt.

3.2. The principle of electromagnetic filtration

An electromagnetic force was generated by passing a DC current through the melt contained in the separation chamber within a crossed uniform magnetic field as shown in Fig. 7. According to references [7–9], the net force exerted by electromagnetic field on a spherical non-metallic particle in melt can be expressed as follows:

$$f_{\mathrm{p}} = -\frac{3}{4}\frac{\pi d_{\mathrm{p}}^3}{6} f \tag{1}$$

where $f = |\vec{B} \times \vec{J}|$ is electromagnetic force acting on a unit volume of the melt, d_{p} is the diameter of the particle.

Drag force acted on the primary iron-rich particle by the Al-Si alloy melt in vertical orientation is [10],

$$R = \varphi \rho d_{\mathrm{p}}^2 v^2 \tag{2}$$

where φ is drag coefficient, R is drag force exerted on the primary iron-rich particle, v is movement velocity in the vertical orientation of the primary iron-rich phase.

The relationship between the moving velocity of the primary iron-rich phase and drag of Al-Si alloy melt is shown in Equation 3,

$$W_{\mathrm{o}} + f_{\mathrm{P}} - R = \frac{\pi d_{\mathrm{p}}^3}{6}\rho_{\mathrm{p}}\frac{\mathrm{d}v}{\mathrm{d}t} \tag{3}$$

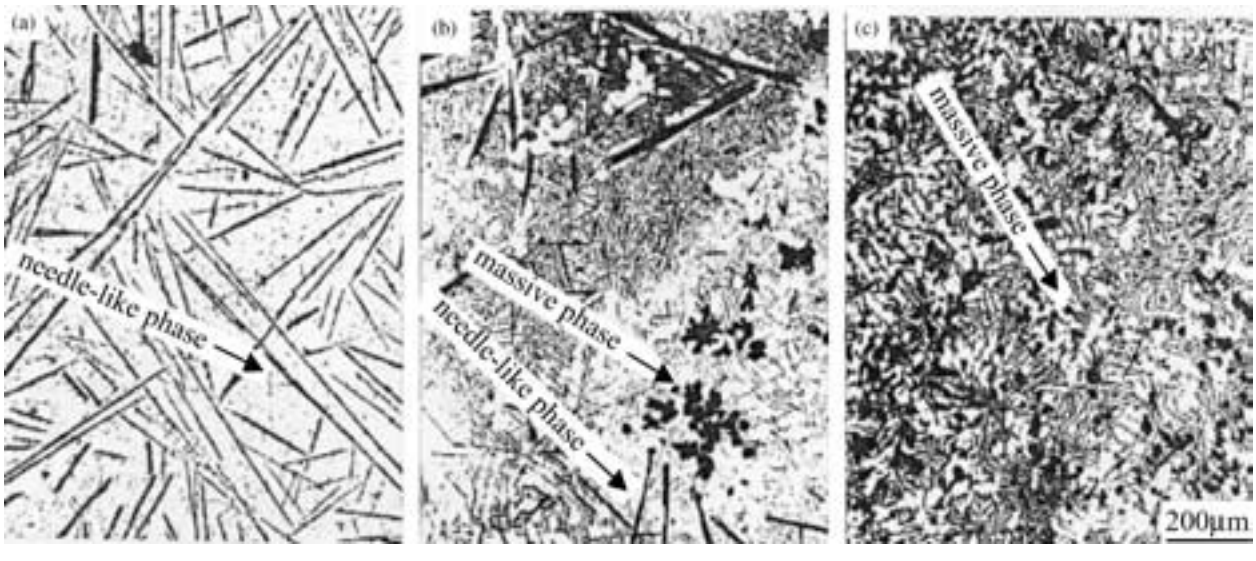

Figure 3 Effect of content of Mn on morphologies of iron-rich phase in the Al-Si-1.2 wt%Fe alloy. (Etched in 20%H_2SO_4 at 70°C for 30 s. The black phase is iron-rich phase.) (a) without Mn, (b) 0.6 wt%Mn, and (c) 1.8 wt%Mn.

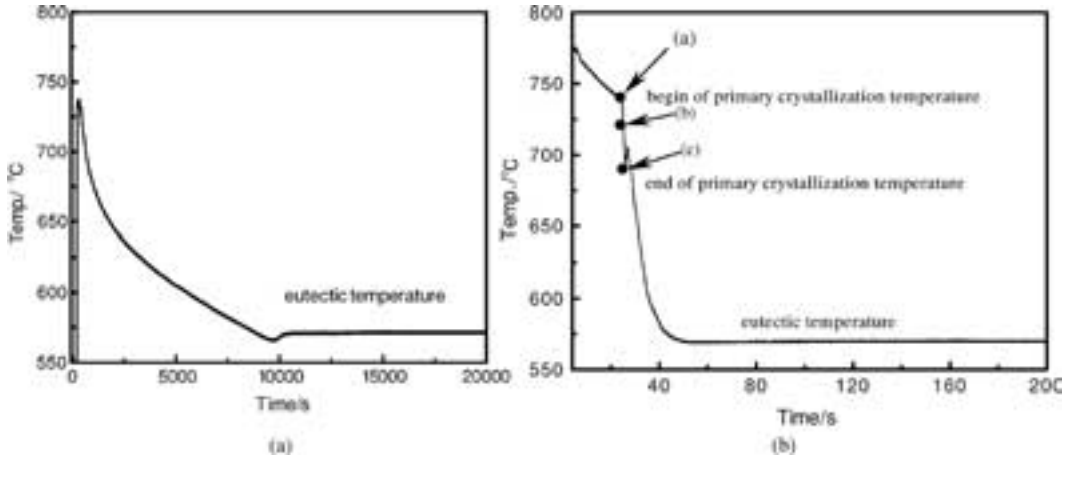

Figure 4 Cooling curve of the alloys: (a) Al-Si-1.2 wt%Fe and (b) Al-Si-1.2 wt%Fe-1.8 wt%Mn.

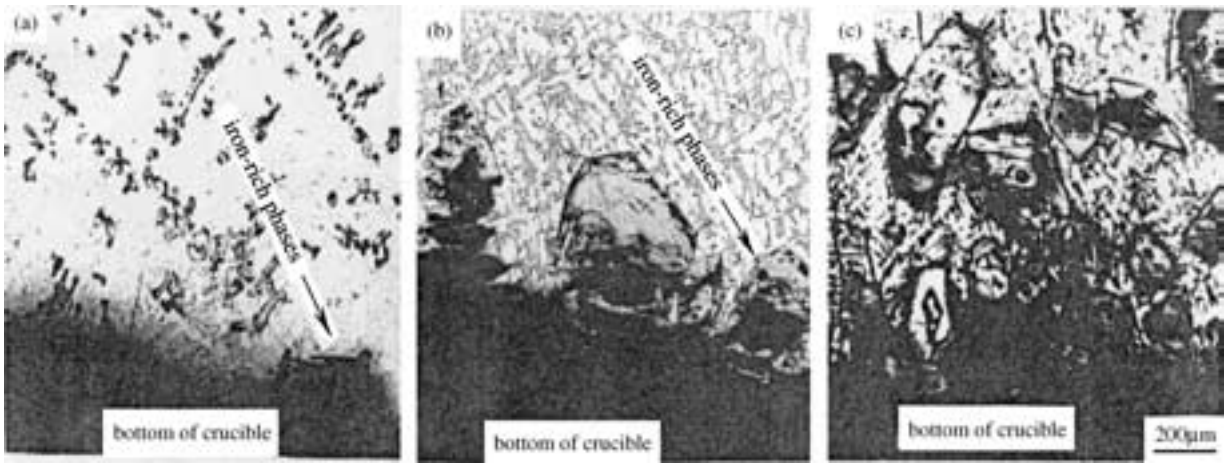

Figure 5 Microstructures after settling at temperatures shown on the cooling curve of Fig. 4b (a), (b) and (c) (Etched in 20%H_2SO_4 at 70°C for 30 s. The black phase is iron-rich phase.)

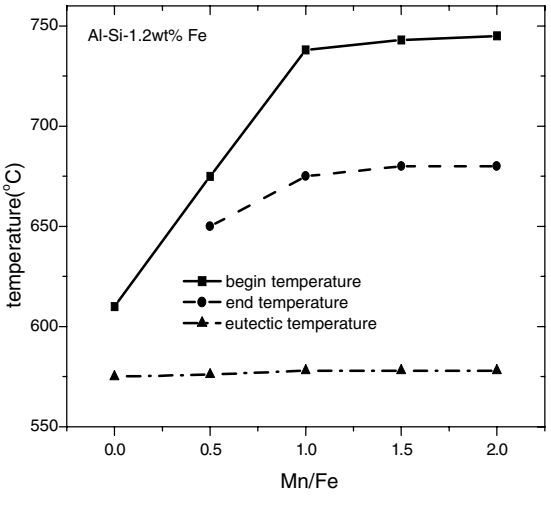

Figure 6 Relation between Mn/Fe ratio and primary crystallization temperature (Al-Si-1.2 wt%Fe).

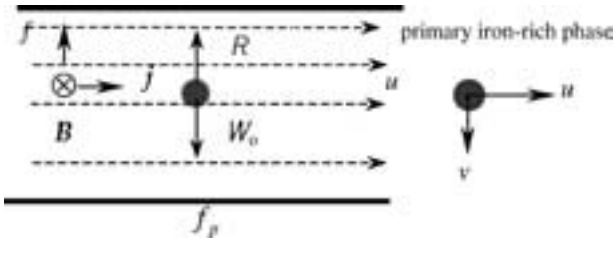

Figure 7 Action forces of primary iron-rich phases while the molten Al-Si alloy is horizontal flow in the single passage of the separation chamber.

where $\frac{dv}{dt}$ is the acceleration of the primary iron-rich phase; W_o is factual gravity of the primary iron-rich phase in the Al-Si alloy melt.

The viscous resistance of the primary iron-rich phase increases as the velocity increases. When forces exerted on the iron-rich phases kept balance, the velocity reached terminal velocity (v_t).

$$v_t = \sqrt{\frac{\pi d_p f}{8\varphi\rho} + \frac{\pi d_p(\rho_p - \rho)}{6\varphi\rho}g} \qquad (4)$$

An acceleration procedure of particle exists while imposing the electromagnetic force on the particle. This procedure can be described by relaxed time τ_p [10].

$$\tau_p = \frac{2\rho_p r^2}{9\rho\mu} \qquad (5)$$

where r is radius of the primary phase, μ is the dynamics viscosity of the melt, ρ_p and ρ are the density of primary phase and the melt, respectively.

According to Table II and Equation 5, the relaxed time of primary iron-rich phases in this experiment is 5.6×10^{-4} s. That is, the relaxed time of primary iron-rich phase of size less than 80 μm is less than 5.6×10^{-4} s. Therefore, in normal conditions, the acceleration procedure of particles can be neglected.

As Reynolds number ($\mathrm{Re} = d_p v_t \rho/\mu$) for small particle in micron size range is less that 1[11,12], φ in Equation 4 is taken to be $3\pi/\mathrm{Re}$ [13]. Equation 4 changes to be,

$$v_t = \frac{d_P^2}{18\mu}\left[(\rho_P - \rho)g + \frac{3}{4}f\right] \qquad (6)$$

In this experiments, the electromagnetic force f ranges from 0 to 2×10^5 N/m^3 ($J = 0$–2.00×10^5 A/m^2 at $B = 1$T, $\mu = 2.54 \times 10^{-3}$ Pa.s). Under such conditions, the calculated value of v_t as a function of f is shown in Fig. 8a. It is seen that the terminal migrating velocity is less than 3–7 mm/s for the primary iron-rich phase smaller than 30 μm.

The terminal natural sedimentation velocity of primary iron-rich phases can be determined by Stokes law, supposing the particle is spherical and molten metal

TABLE II Typical experimental parameters

	r (μm)	μ (mm^2/s)	ρ_p ($\times 10^3$ kg/m^3)	ρ ($\times 10^3$ kg/m^3)
Experiment on the melt	40	1.064 at 720°C	4.0	2.4

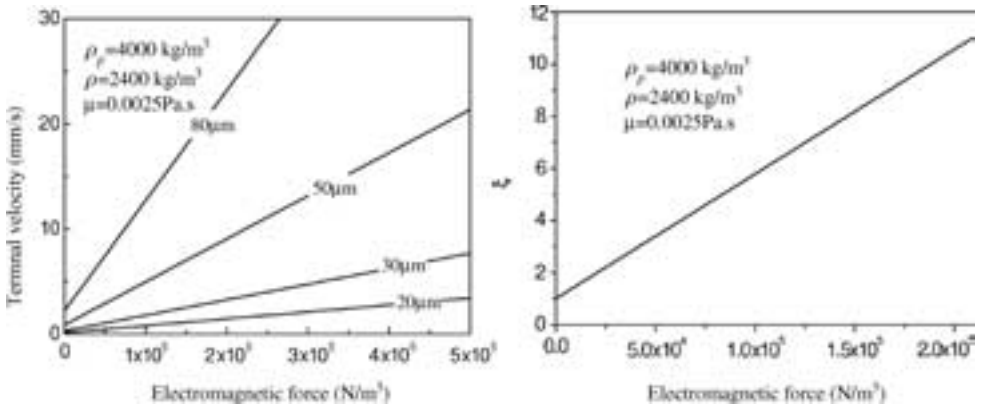

Figure 8 (a) Calculated terminal velocity v_t vs. f (b) the relation between ξ and the electromagnetic force.

remains undisturbed,

$$v_g = \frac{d_p^2 \Delta\rho g}{18\mu} \tag{7}$$

where v_g is the terminal settling velocity; d_p is the diameter of the iron-phase; $\Delta\rho = \rho_p - \rho$, is the density difference between the iron-phase ($\rho_p = 4.0$ kg/m^3) and the melt ($\rho = 2.4$ kg/m^3); $\mu = 2.54 \times 10^{-3}$ Pa.s is the kinetic viscosity of the melt. In order to make a comparison between electromagnetic filtration and natural settling, the ratio (ξ) between the ultimate migrating velocity and the terminal settling velocity is calculated, which gives according to Equations 6 and 7,

$$\xi = 1 + \frac{3f}{4(\rho_P - \rho)g} \tag{8}$$

The values of ξ with the variation of f are given in Fig. 8b. It is seen that the terminal migrating velocity can be up to about 5–8 times higher than the settling velocity. Considering that the magnetic field used in the experiments is rather weak, the terminal migrating rate can be significantly increased in practical cases.

3.3. Model of removal efficiency

The rectangle passages of the electromagnetic separation chamber used in the experiments have large width-to height ratio. Therefore, it is thought that the height of single filtration passage relative to the boundary layer is small. Thus the velocity of the melt depends on the position in the single filtration passage of the separation chamber. At the same time, the moving trajectory of primary iron-rich phases effects its removal efficiency. Thus, trajectory model is analyzed.

The rectangle single filtration passage, $2h$ in height and b in width, is used in the experiment. The following hypotheses are made in the analyses: (1) The flow of the melt inside the single filtration passage of the separation chamber is steady, laminar and uniform; (2) The primary iron-rich phases are considered spherical in shape and there is no interaction between them; (3) The primary iron-rich phases are small enough to neglect the inertial effect; (4) The primary iron-rich phases are entrapped and fixed as soon as they reach the separation chamber walls.

The rectangle passages of the single filtration passage of the separation chamber used in experiments which have large wide-to-height ratio can be thought as two infinitely wide parallel walls with a distance of $2h$. As shown in Fig. 9, the direction of melt flow is specified as the x-axis, and the y-axis is perpendicular to it. The flow equation is as follows [14]:

$$u = \frac{\rho g P^o}{2\mu}(h^2 - y^2) \tag{9}$$

where μ is viscosity of the Al-Si alloy melt, P^o is pressure loss of unit Al-Si alloy melt, u is horizontal velocity of Al-Si alloy melt, $2h$ is the height of the single filtration passage of the separation chamber.

It is obvious that distribution of flow velocity is parabola, and when $y = 0$, flow velocity is the most,

$$u_M = \frac{\rho g P^o}{2\mu} h^2 \tag{10}$$

It can be obtained from Equations 9 and 10 that,

$$u = u_M \left[1 - \left(\frac{y}{h}\right)^2\right] \tag{11}$$

where u_M is the maximum flow velocity of the melt. The x- and y-component of the primary iron-rich phases are

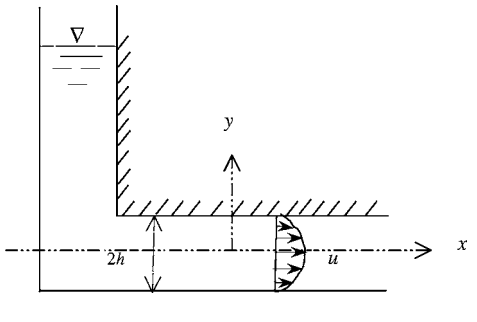

Figure 9 Distribution of the melt fluid velocity in a single passage of the separation chamber.

denoted by u_x and u_y, respectively.

$$u_x = u_M\left(1 - \frac{y^2}{h^2}\right) = \frac{dx}{dt} \tag{12}$$

$$u_y = v_t = \frac{dy}{dt} \tag{13}$$

As a result,

$$\frac{dx}{dy} = \frac{u_x}{u_y} = \frac{u_M\left(1 - \frac{y^2}{h^2}\right)}{v_t} \tag{14}$$

When integrating the above equation, it can be obtained that,

$$x = \frac{u_M y - \frac{u_M y^3}{3h^2} + \frac{2}{3}hu_M}{v_t} \tag{15}$$

The initial y position of the primary iron-rich phases, which arrive at an arbitrary x position, can be deduced from Equation 9. Apparently, the primary iron-rich phases below the y position have already reached the wall. Therefore, the removal efficiency of the primary iron-rich phases can be expressed by,

$$\eta = \int_{-h}^{y} u_x.b\,dy \Big/ \int_{-h}^{h} u_x.b\,dy \tag{16}$$

i.e.

$$\eta = \frac{3h^2y - y^3 + 2h^3}{4h^3} \tag{17}$$

It can be obtained from Equations 15 and 17 that,

$$\eta = \frac{3xv_t}{4hu_M} \tag{18}$$

By combining Equation 6 with Equation 18, the effects of x, $2h$, f and u_M on η can be found. For Al-Si alloy melt, the effects of x, $2h$, f and u_M on η are shown in Fig. 10 when μ, ρ, ρ_p are taken to be 2.54×10^{-3} Pa.s, 2.4×10^3 kg/m^3, 4.0×10^3 kg/m^3, respectively. It is indicated that the removal efficiency increases with the

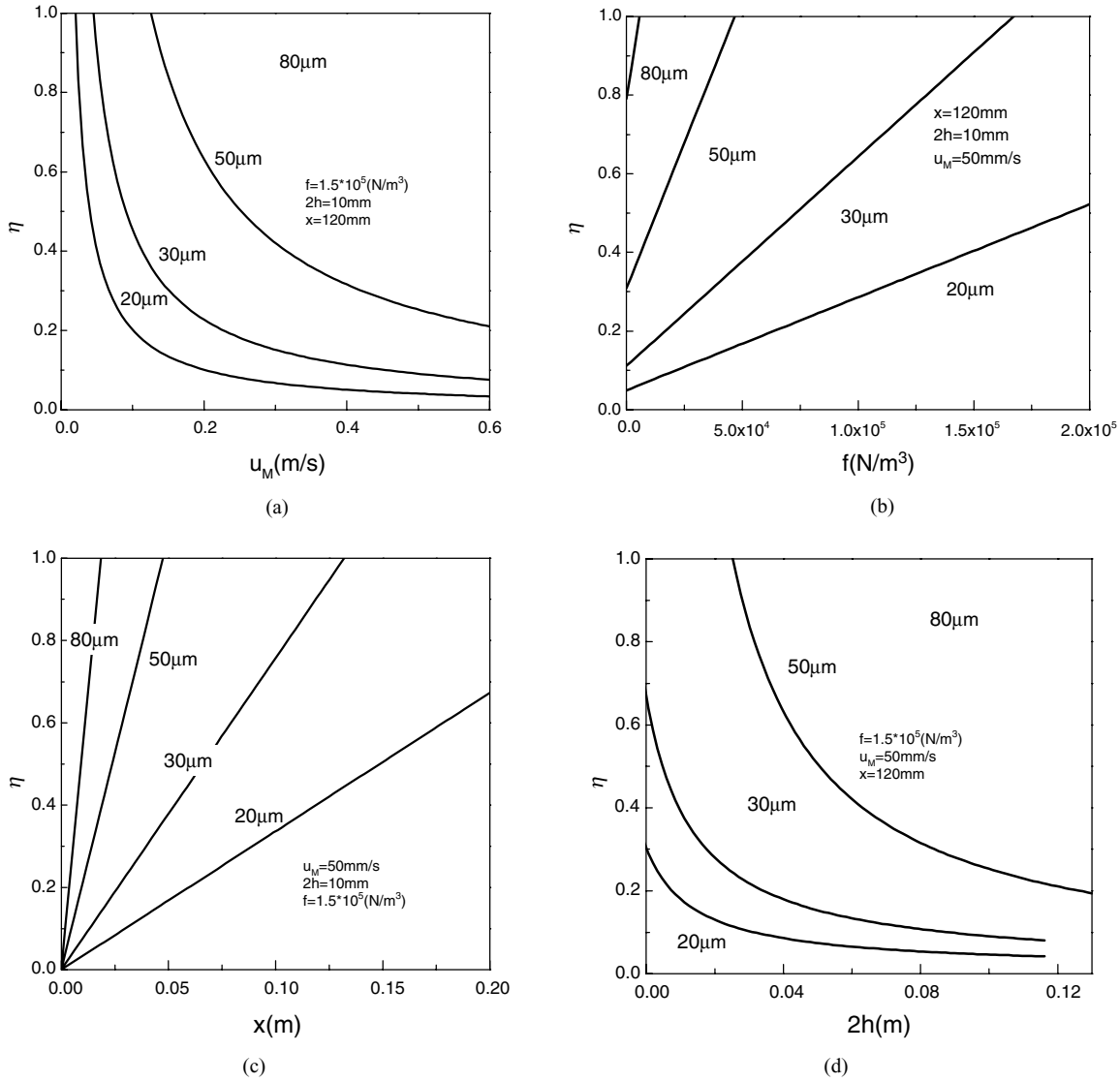

Figure 10 Removal efficiency vs. technological parameter: (a) fluid velocity(u_M), (b) electromagnetic force (f), (c) height of the single filtration passage of the separation chamber ($2h$), and (d) action length of electromagnetic force (x).

increment of electromagnetic force (f), action length of electromagnetic force (x), particle size (d_p) and decreases with the increment of height of single filtration passage ($2h$) and velocity of the melt (u_M). From Fig. 10b, it is seen that the removal efficiency of the iron-phases larger that 30 μm can reach above 90% when f is equal to 1.5×10^5 N/m^3. From Fig. 10c, it is seen that the removal efficiency of the iron-rich phases larger that 30 μm can reach 100% when the height of the separation chamber is 5 mm.

The above analysis is concerned within a single passage of the separation chamber. Since the case of a complete separation chamber (multi-passages) is like that of a single passage, the obtained results can be used as an aid to design the structure of the electromagnetic filters and to predict the removal efficiency.

3.4. Electromagnetic filtration of primary iron-phases from Al-Si alloy melt

According to the calculated results, the process parameters of electromagnetic filtration are: fluid velocity(u_M) is 50 mm/s; electromagnetic force (f) is 1.5×10^5 N/m^3; height of the single filtration passage of the separation chamber ($2h$) is 5 mm; action length of electromagnetic force (x) is 120 mm. The results of electromagnetic filtration of iron-rich phases from Al-Si alloy are shown in Fig. 11. Fig. 11a and b are metallographs of the alloy solidified in the single filtration passage of the separation chamber. As shown in Fig. 11a and b, a large amount of the primary iron-rich phases were captured by the separation chamber when the melt flowed through the chamber. Fig. 11c, demonstrates that there are no primary iron-rich phases in the microstructure after electromagnetic filtration.

It can be seen in Fig. 12 that when other parameters were kept the same, a large electromagnetic force is more efficient in removing primary iron-rich phases than a small one. There are no primary iron-rich phases in Fig. 12d while some primary iron-rich particles can be found in Fig. 12a, b, and c. At the same time, as shown Fig. 13, a slow fluid velocity is more efficient in removing primary iron-rich phases than a rapid one. There are no primary iron-rich phases in Fig. 13a while some primary iron-rich particles can be found in Fig. 13b, c, and d.

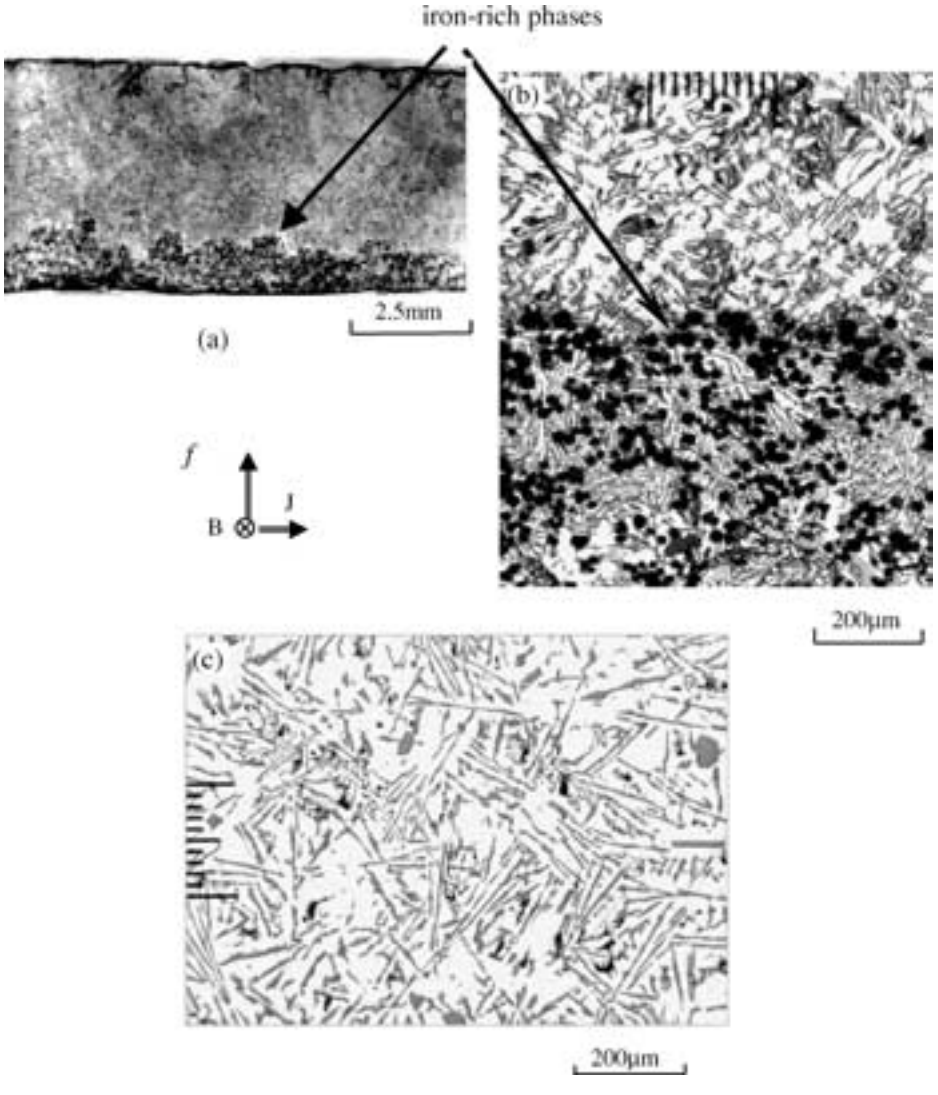

Figure 11 Electromagnetic filtration of iron-rich phases from Al-11.7 wt%Si-1.2 wt%Fe-1.8 wt%Mn alloy (Etched in 20%H_2SO_4 at 70°C for 30 s. The black phase is iron-rich phase.) ($f = 1.5 \times 10^5$ N/m^3, $u_M = 50$ mm/s, $x = 120$ mm, $2h = 5$ mm): (a) macrostructure of the metal in the single filtration passage of the separation chamber (b) enlarged detail indicated by frame in (a), and (c) metallograph of processed alloy metal.

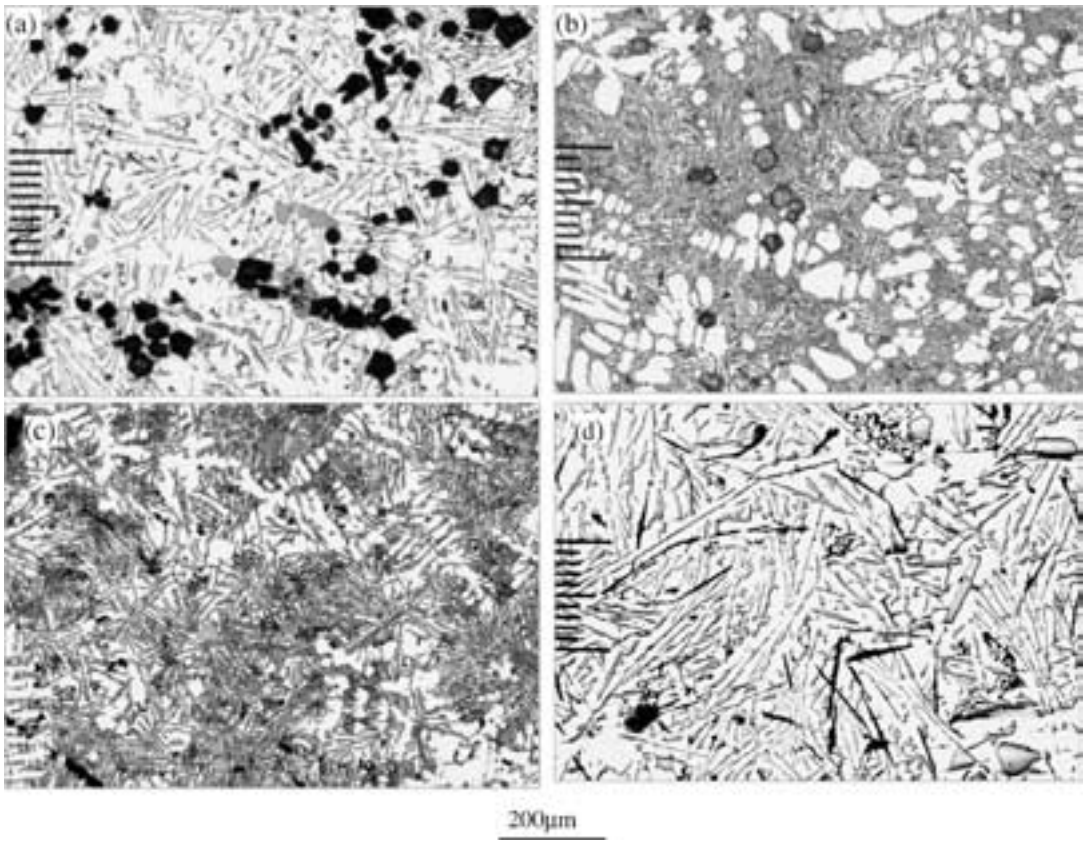

Figure 12 Influence of electromagnetic force on separation effect (Etched in 20%H_2SO_4 at 70°C for 30 s. The black phase is iron-rich phase.) (a) $f = 0$, (b) $f = 0.5 \times 10^5$ N/m^3, (c) $f = 1.0 \times 10^5$ N/m^3, and (d) $f = 1.5 \times 10^5$ N/m^3 ($u_M = 50$ mm/s, $x = 120$ mm, $2h = 5$ mm).

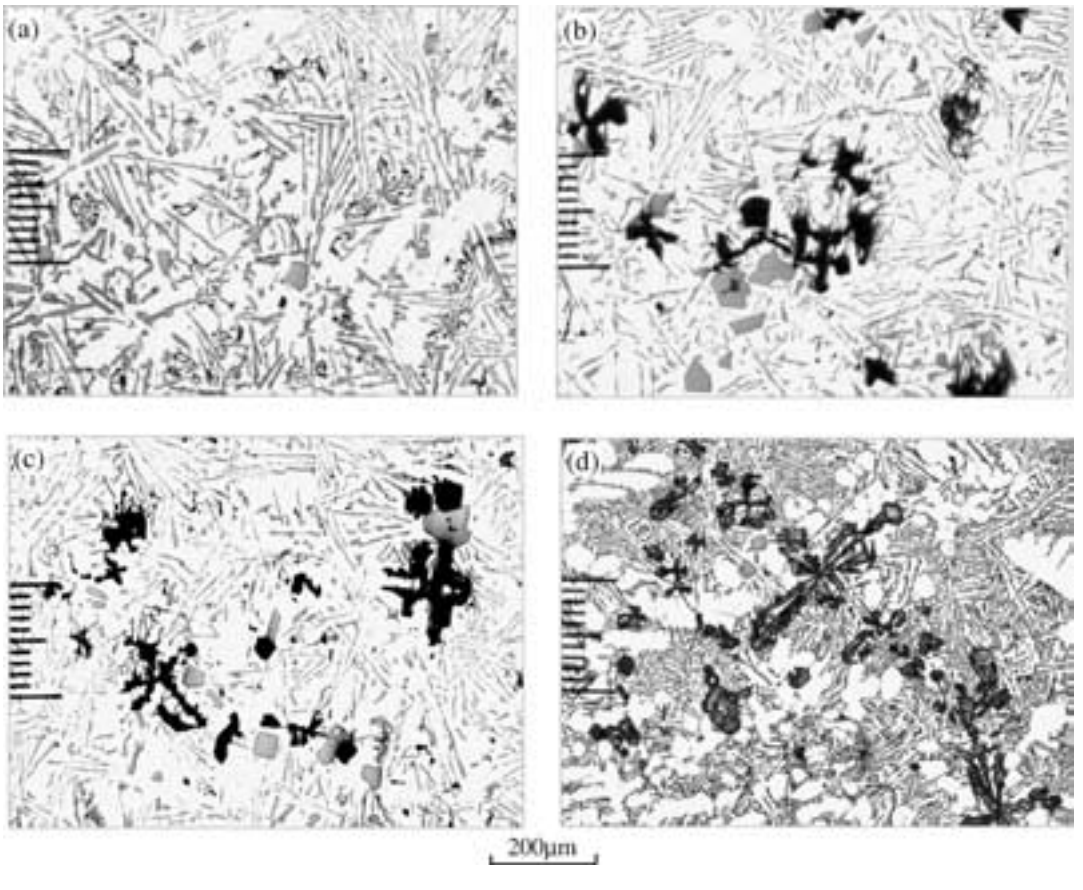

Figure 13 Influence of melt velocity on separation effect (Etched in 20%H_2SO_4 at 70°C for 30 s. The black phase is iron-rich phase.) (a) 50 mm/s, (b) 65 mm/s, (c) 80 mm/s, and (d) 95 mm/s ($f = 1.5 \times 10^5$ N/m^3, $x = 120$ mm, $2h = 5$ mm).

TABLE III Fe content before and after electromagnetic treatment

Before filtration (wt%)		After electromagnetic filtration (wt%)		
Fe	Mn	Fe	Mn	Parameters
1.18	1.85	0.54	0.33	$u_M = 50$ mm/s, $f = 1.0 \times 10^5$ N/m^3, $2h = 5$ mm
1.20	1.81	0.41	0.26	$u_M = 50$ mm/s, $f = 1.5 \times 10^5$ N/m^3, $2h = 5$ mm
1.21	1.72	0.86	0.55	$u_M = 80$ mm/s, $f = 1.5 \times 10^5$ N/m^3, $2h = 5$ mm

Fe and Mn content in the alloy before and after electromagnetic filtration are listed in Table III. Fe reduction in Table III also indicates that larger electromagnetic force and slow fluid velocity are favorable to the removal of primary iron-rich phases. The iron content in the cast ingot decreases from 1.20% to 0.41% by electromagnetic filtration when the fluid velocity (u_M) is 50 mm/s, the electromagnetic force (f) is 1.5×10^5 N/m^3, the height of the single filtration passage of the separation chamber ($2h$) is 5 mm, and the action length of electromagnetic force (x) is 120 mm. The removal efficiency of the primary iron-rich particles larger than 30 μm is calculated by Equation 18 to reach 100%, which is in agreement with the experimental results that there are no primary iron-rich particles larger than 30 μm in Fig. 11c. Therefore, the composition of the alloy can meet the demand for casting after electromagnetic filtration.

4. Conclusions

1. It has been found that primary iron-rich phases are formed primarily in the Al-Si 1.2 wt%Fe melt after adding Mn. They appear as massive particles with size of 30–80 μm.

2. The primary iron-rich phases can be removed from Al-Si alloy melt by applying an electromagnetic force on molten aluminum contained in a separation chamber, and are captured by the separation chamber while the melt is in continuous horizontal flow.

3. The method of electromagnetic filtration of primary iron-rich phases is highly efficient and amenable for continuous flowing melt in contrast with natural settling and filtration.

4. The iron content in the cast ingot decreases from 1.20% to 0.41% by electromagnetic filtration and the composition of the alloy can meet the demand for casting.

Acknowledgments

This project was supported by the National Science Foundation of China (No. 50271042) and the Research Fund for the Doctoral Program of Higher Education.

References

1. P. N. CREPEAU, *AFS Trans.* **103** (1995) 360.
2. W. B. FANG, Y. H. GENG and R. M. YE, *Foundry Techn.* **2** (1996) 5 (in Chinese).
3. HIROMI MATSUBARA and MASARU NAKANISHI, *J. Jpn. Inst. Light Met.* **48** (1998) 93.
4. JOON-PYOU PARK, KENSUKE SASSA and SHIGEO ASAI, *J. Jpn. Inst. Met.* **59** (1995) 312.
5. JEONG-HO KIM and EUI-PAK YOON, *J. Mater. Sci. Lett.* **19** (2000) 253.
6. N. EL-KADDAH, A. D. PATEL and T. T. NATARAJAN, *J. Met.* **5** (1995) 46.
7. DANIEL LEENOV and ALEXANDER KOLIN, *J. Chen. Phys.* **22** (1954) 683.
8. P. H. MARTY, A. ALEMANY, RICOUR. and C. H. VIVES, *Prog. Astron. Aeron.* **84** (1983) 402.
9. PH. MARTY and A. ALEMANY, "Theoretical and Experimental Aspects of Electromagnetic Separation, Metallurgical Applications of Magnetohydrodynamics, in Proceedings of a Symposium of the International Union of Theoretical and Applied Mechanics" (Sponsored by: Int Union of Theoretical & Applied Mechanics, Goteborg, Swed Metals Soc., 1984) p. 245.
10. S. Y. BO, "Two-Phase Flow" (National Defence Industry Press, Beijing, 1985) p. 165 (in Chinese).
11. JOON-PYOU PARK, ATUSI MORHIRA and KENSUKE SASSA, *Tetsu-to-Hagané* **80** (1994) 31 (in Japanese).
12. SHOJI TANGUCHI and J. KEITH BRIMACOMBE, *Tetsu-to-Hagané* **80** (1994) 24 (in Japanese).
13. Q. L. TONG, "Theory of Two-Phase Flow" (Beijing, Metallurgical Industry Press, 1982) p. 50 (in Chinese).
14. C. G. ZHANG, "Drodynamics" (Hgher Education Press, Beijing, 1982) p. 443 (in Chinese).

Received 22 October 2002
and accepted 5 August 2003